Inorg. Chem. **2009**, *48*, 598−606

Gas-Phase Fragmentation of Polyoxotungstate Anions

Michelle T. Ma,*,†,‡ Tom Waters,*,†,‡ Karin Beyer,† Rosemary Palamarczuk,† Peter J. S. Richardt,† Richard A. J. O'Hair,†,‡ and Anthony G. Wedd†,‡

School of Chemistry, University of Melbourne, Victoria 3010, Australia, and Bio21 Institute of Molecular Science and Biotechnology, The University of Melbourne, Victoria 3010, Australia

Received August 27, 2008

A series of phospho-polyoxotungstate anions was transferred to the gas phase via electrospray ionization (ESI), and the anions' fragmentation was examined by collision-induced dissociation (CID). The anions included $[PW_{12}O_{40}]^{3-}$, $[P_2W_{18}O_{62}]^{6-}$, and $\{Co_4(H_2O)_2][PW_9O_{34}]_2\}^{10-}$ as well as lacunary and metal-substituted derivatives such as $[PW_{11}O_{39}]^{7-}$ and $[MPW_{11}O_{39}]^{5-}$ (M = Co^{II}, Ni^{II}, Cu^{II}). Common species observed in the mass spectra arose from protonation and alkali metal cationization of the precursor ions. Additional species arising from the formal loss of oxide from the precursor species were also observed, presumably formed via protonation and the loss of an oxo ligand as water. These processes of protonation/cationization and the loss of water both led to species with reduced gas-phase anionic charges, and their formation appears to be driven by the enhanced effects of Coulombic repulsion in the desolvated species generated during transfer to the gas phase via ESI. Fragmentation of selected species was examined by multistage mass spectrometry experiments employing CID. Fragmentation occurred via multiple reaction channels, leading to pairs of complementary product anions whose total stoichiometry and charge matched those of the precursor anion. For example, $[PW_{12}O_{40}]^{3-}$ fragmented to give pairs of product ions of general formulas $[W_xO_{3x+1}]^{2-}$ and $[PW_{12-x}O_{39-3x}]^{-}$ ($x = 6-9$), with the most intense pair being $[W_6O_{19}]^{2-}$ and $[PW_6O_{21}]^{-}$. Similar ions were also observed for fragmentation of $[P_2W_{18}O_{61}]^{4-}$ (derived from the loss of water from $[P_2W_{18}O_{62}]^{6-}$). The lacunary and M^{II}-substituted lacunary systems fragmented via related pathways, with the latter generating additional fragment ions due to the presence of M^{II}. These results highlight the usefulness of ESI-MS in the characterization of complex polyoxometalate anion clusters.

Introduction

Polyoxometalates are metal oxide cluster anions containing early transition metals in their highest oxidation states, typically Mo^{VI}, W^{VI}, and V^{V}. They have been studied extensively due to their interesting structural, catalytic, and redox properties, and their application in areas as diverse as catalysis, analytical chemistry, and medicine.[1−4] The clusters are typically assembled from edge- and corner-shared distorted MO_6 pseudo-octahedral units, and the most stable adopt high-symmetry, quasi-spherical structures. Well known and extensively studied examples include the Lindquist $[W_6O_{19}]^{2-}$, the Keggin $[PW_{12}O_{40}]^{3-}$, and the Dawson $[P_2W_{18}O_{62}]^{6-}$ anions.[1−3] The latter two feature the "heteroatoms" P^{V} as part of a central tetrahedral PO_4 unit (Figure 1). Under basic conditions, the formal removal of a WO^{4+} unit from the Keggin and Dawson structures gives rise to "lacunary" structures $[PW_{11}O_{39}]^{7-}$ and $[P_2W_{17}O_{61}]^{10-}$, respectively, with a single metal vacancy in the cluster framework. The vacant metal site in these clusters can be filled by other transition metal ions such as Co^{II} to give derivatives such as $[Co^{II}PW_{11}O_{39}]^{5-}$ and $[Co^{II}P_2W_{17}O_{61}]^{8-}$.[1−4] Finally, the Tourné "sandwich" complex $[Co_4(PW_9O_{34})_2]^{10-}$ is assembled from four Co^{II} ions sandwiched between two

* Authors to whom correspondence should be addressed. Tel.: 61 3 8344 2411. Fax: 61 3 9347 5180. E-mail: waterst@unimelb.edu.au (T.W.), mtma@unimelb.edu.au (M.T.M.).

† School of Chemistry.

‡ Bio21 Institute of Molecular Science and Biotechnology.

(1) Pope, M. T. *Heteropoly and Isopolyoxometalates*; Springer-Verlag: Berlin, 1983.

(2) Hill, C. L. *Chem. Rev.* **1998**, *98*, 1–388; thematic issue devoted to polyoxometalate chemistry.

(3) Hill, C. L. Polyoxometalates: Reactivity. In *Comprehensive Coordination Chemistry-II: From Biology to Nanotechnology*; Elsevier: Oxford, U.K., 2004; Vol. *4*, pp 679−759.

(4) Hill, C. L. *J. Mol. Catal. A* **2007**, *262*, 2–6.

(5) Pope, M. T. Polyoxometalates: Synthesis and Structure. In *Comprehensive Coordination Chemistry-II: From Biology to Nanotechnology*; Elsevier: Oxford, U.K., 2004; Vol. *4*, pp 635−678.

10.1021/ic8016326 CCC: $40.75
Published on Web 12/15/2008

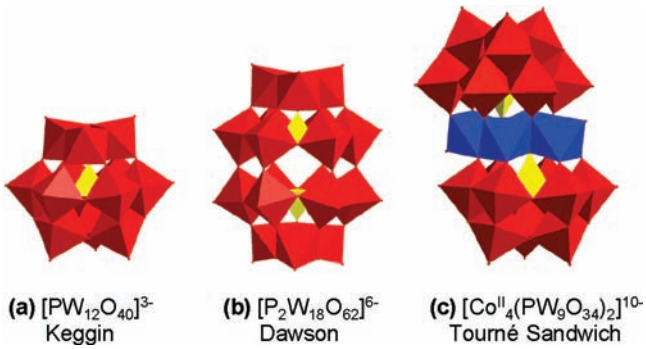

Figure 1. Structures of classic polyoxometalate anions examined: (a) the Keggin anion $[PW_{12}O_{40}]^{3-}$, (b) the Dawson anion $[P_2W_{18}O_{62}]^{6-}$, and (c) the Tourné sandwich anion $[Co^{II}_4(PW_9O_{34})_2]^{10-}$.

$PW_9O_{34}^{9-}$ fragments, the latter related to the Keggin anion by removal of a W_3 "cap" unit (Figure 1c).

More recent synthetic achievements have provided hundreds of anions of greater complexity.[5] However, their detailed molecular characterization continues to present challenges. One aspect relates to the concentration, pH, and solvent-dependent equilibria that can exist in solution.[1,5] X-ray crystallography and NMR have provided key insights, but difficulties remain. These include the characterization of intermediates relevant to the assembly of larger clusters. To this end, mass spectrometry offers the potential of providing detailed insights into the molar mass and stoichiometry of species present in solution. Important developmental work employed fast atom bombardment to examine a range of species.[6−10] However, the results were hampered by the observation of a single charge state only (a characteristic of the technique), resolution problems induced by the broad isotope patterns of molybdenum- and tungsten-containing clusters, and the significant degree of fragmentation observed experimentally.

The advent of electrospray ionization mass spectrometry (ESI-MS) has transformed the analysis of complex inorganic ions.[11] The technique has been used recently to analyze a range of characterized polyoxoanions, as well as complex mixtures of oxoanions (present due to pH and concentration-dependent equilibria).[12−21] The approach has now been extended to larger and more complex species and to their identification in synthetic media.[22−27] A common feature is the observation of charge reduction during the electrospray process, presumably driven by the instability of highly charged clusters due to the Coulombic repulsion in the bare clusters following desolvation.[28−31] The charge reduction commonly involves (i) ion association to form gas-phase ion clusters comprised of multiply charged polyoxoanions and available counterions or (ii) protonation of oxo ligands of the polyoxoanion cluster to form hydroxo ligands, which is often followed by a loss of water from the cluster framework. The net result of the latter process is the formal removal of O^{2-} from the cluster.[21,32−34]

Few studies have reported the gas fragmentation phenomena of these clusters.[22,35] Fragmentation provides insight into the favored decomposition pathways of gas-phase clusters and, by extension, might also provide insights into the intermediates relevant to their formation. Fragmentation of the polyoxoanions $[M_6O_{19}]^{2-}$, $[Mo_8O_{26}]^{4-}$, $[W_{10}O_{32}]^{4-}$, $[PW_{12}O_{40}]^{3-}$, and $[SiM_{12}O_{40}]^{4-}$ (M = Mo, W) has been examined.[35] $[M_6O_{19}]^{2-}$ (M = Mo, W), for example, fragmented to $[M_4O_{13}]^{2-}$ and $[M_3O_{13}]^{2-}$, presumably via loss of consecutive neutral MO_3 fragments or of M_2O_6 and M_3O_9, respectively. However, although some larger and more complex clusters have also been examined by ESI-MS,[22−27] a systematic study of the gas-phase fragmentation of polyoxometalate clusters has yet to appear.

The present work defines the collision-induced dissociation (CID) fragmentation reactions of a series of ions derived from ESI-MS spectra of a set of well-defined classic polyoxotungstate clusters based upon the Keggin $[PW_{12}O_{40}]^{3-}$, Dawson $[P_2W_{18}O_{62}]^{6-}$, and Tourné $[Co_4(PW_9O_{34})_2]^{10-}$ anions

(6) Finke, R. G.; Droege, M. W.; Cook, J. C.; Suslick, K. S. *J. Am. Chem. Soc.* **1984**, *106*, 5750–5751.
(7) Suslick, K. S.; Cook, J. C.; Rapko, B.; Droege, M. W.; Finke, R. G. *Inorg. Chem.* **1986**, *25*, 241–243.
(8) Trovarelli, A.; Finke, R. G. *Inorg. Chem.* **1993**, *32*, 6034–6039.
(9) Abrams, M. J.; Costello, C. E.; Shaikh, S. N.; Zubieta, J. *Inorg. Chim. Acta* **1991**, *180*, 9–11.
(10) Wasfi, S. H.; Costello, C. E.; Rheingold, A. L.; Haggerty, B. S. *Inorg. Chem.* **1991**, *30*, 1788–1792.
(11) Colton, R.; Traeger, J. C. *Inorg. Chim. Acta* **1992**, *201*, 153–155.
(12) Deery, M. J.; Howarth, O. W.; Jennings, K. R. *J. Chem. Soc., Dalton Trans.* **1997**, 4783–4788.
(13) Walanda, D. K.; Burns, R. C.; Lawrance, G. A.; Von Nagy-Felsobuki, E. I. *Inorg. Chem. Commun.* **1999**, *2*, 487–489.
(14) Walanda, D. K.; Burns, R. C.; Lawrance, G. A.; von Nagy-Felsobuki, E. I. *J. Chem. Soc., Dalton Trans.* **1999**, *3*, 311–322.
(15) Walanda, D. K.; Burns, R. C.; Lawrance, G. A.; von Nagy-Felsobuki, E. I. *Inorg. Chim. Acta* **2000**, *305*, 118–126.
(16) Walanda, D. K.; Burns, R. C.; Lawrance, G. A.; Von Nagy-Felsobuki, E. I. *J. Cluster Sci.* **2000**, *11*, 5–28.
(17) Easterly, C. E.; Hercules, D. M.; Houalla, M. *Appl. Spectrosc.* **2001**, *55*, 1665–1670.
(18) Easterly, C. E.; Hercules, D. M.; Houalla, M. *Appl. Spectrosc.* **2001**, *55*, 1671–1675.
(19) Truebenbach, C. S.; Houalla, M.; Hercules, D. M. *J. Mass Spectrom.* **2000**, *35*, 1121–1127.
(20) Sahureka, F.; Burns, R. C.; von Nagy-Felsobuki, E. I. *Inorg. Chem. Commun.* **2002**, *5*, 23–27.
(21) Sahureka, F.; Burns, R. C.; von Nagy-Felsobuki, E. I. *Inorg. Chim. Acta* **2003**, *351*, 69–78.
(22) Nellutla, S.; Van Tol, J.; Dalal, N. S.; Bi, L.-H.; Kortz, U.; Keita, B.; Nadjo, L.; Khitrov, G. A.; Marshall, A. G. *Inorg. Chem.* **2005**, *44*, 9795–9806.
(23) Streb, C.; Long, D.-L.; Cronin, L. *Chem. Commun.* **2007**, 471–473.
(24) Pradeep, C. P.; Long, D.-L.; Koegerler, P.; Cronin, L. *Chem. Commun.* **2007**, 4254–4256.
(25) Miras Haralampos, N.; Long, D.-L.; Kogerler, P.; Cronin, L. *Dalton* **2008**, 214–221.
(26) Long, D.-L.; Streb, C.; Song, Y.-F.; Mitchell, S.; Cronin, L. *J. Am. Chem. Soc.* **2008**, *130*, 1830–1832.
(27) Fay, N.; Bond, A. M.; Baffert, C.; Boas, J. F.; Pilbrow, J. R.; Long, D.-L.; Cronin, L. *Inorg. Chem.* **2007**, *46*, 3502–3510.
(28) Wang, L.-S.; Wang, X.-B. *J. Phys. Chem. A* **2000**, *104*, 1978–1990.
(29) Yang, X.; Waters, T.; Wang, X.-B.; O'Hair, R. A. J.; Wedd, A. G.; Li, J.; Dixon, D. A.; Wang, L.-S. *J. Phys. Chem. A* **2004**, *108*, 10089–10093.
(30) Zhai, H.-J.; Huang, X.; Waters, T.; Wang, X.-B.; O'Hair, R. A. J.; Wedd, A. G.; Wang, L.-S. *J. Phys. Chem. A* **2005**, *109*, 10512–10520.
(31) Waters, T.; Huang, X.; Wang, X.-B.; Woo, H.-K.; O'Hair, R. A. J.; Wedd, A. G.; Wang, L.-S. *J. Phys. Chem. A* **2006**, *110*, 10737–10741.
(32) Mayer, C. R.; Roch-Marchal, C.; Lavanant, H.; Thouvenot, R.; Sellier, N.; Blais, J.-C.; Sécheresse, F. *Chem.—Eur. J.* **2004**, *10*, 5517–5523.
(33) Boglio, C.; Lenoble, G.; Duhayon, C.; Hasenknopf, B.; Thouvenot, R.; Zhang, C.; Howell, R. C.; Burton-Pye, B. P.; Francesconi, L. C.; Lacôte, E.; Thorimbert, S.; Malacria, M.; Afonso, C.; Tabet, J.-C. *Inorg. Chem.* **2006**, *45*, 1389–1398.
(34) Laurencin, D.; Thouvenot, R.; Boubekeur, K.; Proust, A. *Dalton* **2007**, 1334–1345.
(35) Lau, T.-C.; Wang, J.; Guevremont, R.; Siu, K. W. M. *Chem. Commun.* **1995**, 977–978.

Scheme 1. Overview of the Keggin, Dawson, and Tourné Clusters Studied, and the Relationship between the Parent, Lacunary, and Metal-Substituted Species Observed via Electrospray Mass Spectrometry and Examined via Collision-Induced Dissociation

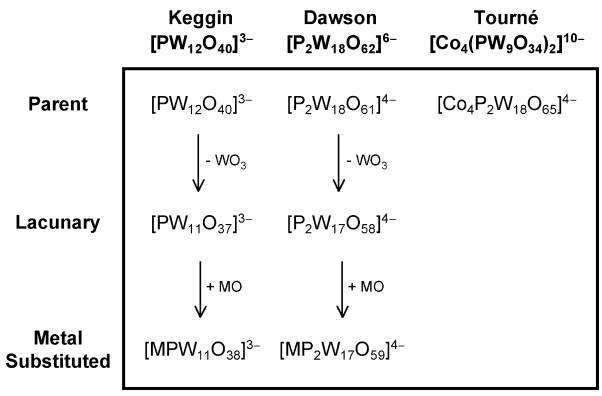

(Figure 1). The ions examined are summarized in Scheme 1 and include lacunary and metal-substituted derivatives. These particular ions were chosen for further fragmentation studies in order to make comparisons between a similar series of ions of the same charge state, containing the same transition metal (W^{VI}) and with the same heteroatom (P^{V}). In each case, the "bare" metal-oxide clusters without the presence of other cations such as H^+ or K^+ were chosen for fragmentation studies. Trends in the fragmentation pathways observed and common fragmentation ions generated are described. The results are useful in defining further the scope of ESI-MS and CID in the characterization of polyoxometalate clusters.

Experimental Section

Synthesis. Polyoxometalate salts were synthesized by literature procedures as follows: $Na_7[PW_{11}O_{39}]\cdot 15-20H_2O$,[36] $K_5[(H_2O)Co^{II}PW_{11}O_{39}]\cdot 15H_2O$,[37] $K_5[(H_2O)Ni^{II}PW_{11}O_{39}]\cdot 14H_2O$,[38] $K_5[(H_2O)Cu^{II}PW_{11}O_{39}]\cdot 23H_2O$,[39] $K_4[(H_2O)Fe^{III}PW_{11}O_{39}]\cdot 14H_2O$,[40] $K_6[P_2W_{18}O_{62}]$,[41] $K_{10}[P_2W_{17}O_{61}]\cdot 15H_2O$,[42] $K_8[(H_2O)M^{II}P_2W_{17}O_{61}]\cdot 16-17H_2O$ (M = Co, Ni, Cu), [42]$K_{10}[(H_2O)_2M_4P_2W_{18}O_{68}]\cdot 20H_2O$ (M = Co, Zn).[41]

Mass Spectrometry. Mass spectra were recorded in the negative ion mode on an Agilent 6510 Q-TOF LC/MS mass spectrometer coupled to an Agilent 1100 LC system (Agilent, Palo Alto, CA). Data were acquired and reference mass corrected via a dual-spray electrospray ionization source, using the factory-defined calibration procedure. Each scan or data point on the total ion chromatogram is an average of 10 000 transients, producing a scan every second. Spectra were created by averaging the scans across each peak. Mass spectrometer conditions: drying gas flow, 7 L/min; nebulizer, 30 psi; drying gas temperature, 350 °C; V_{cap}, 4000 V; skimmer, 65 V; OCT R_fV, 750 V; scan range acquired, 100−3000 *m/z*. Sample solutions were made to approximately 2 mg/mL in water and transferred to the electrospray source via an autosampler. The coeluent was 50:50 MeCN/H_2O containing 0.1% formic acid. (Formic acid was added to aid protonation of the gas-phase species. Protonated gas-phase species subsequently lost water, forming "bare" multiply charged anions. These bare anions were chosen to undergo CID.) CID experiments were performed using Ar as the target gas. Fragmentor and collisional energy voltages were respectively 120 and 32 V ($[PW_{12}O_{40}]^{3-}$), 150 and 20 V ($[PW_{11}O_{37}]^{3-}$), 170 and 25 V ($[MPW_{11}O_{38}]^{3-}$ M = Co, Ni, Cu), 120 and 50 V ($[MPW_{11}O_{38}]^{2-}$ M = Fe), 120 and 20 V ($[P_2W_{18}O_{61}]^{4-}$), 150 and 20 V ($[P_2W_{17}O_{58}]^{4-}$), 150 and 12 V ($[MP_2W_{17}O_{59}]^{4-}$ M = Co, Ni, Cu), and 170 and 20 V ($[P_2W_{18}M_4O_{65}]^{4-}$ M = Zn, Co).

Tungsten-containing ions display distinctive isotopomer patterns due to the relative abundances of the naturally occurring isotopes of tungsten (^{180}W, 0.3; ^{182}W, 85.7; ^{183}W, 46.6; ^{184}W, 100; ^{186}W, 93.1% relative abundance). This allows the charge of ions to be assigned on the basis of peak separation and facilitates the assignment of ion stoichiometry via comparison of experimental and theoretical isotopomer patterns (Figure S1, Supporting Information). The *m/z* values quoted in the text are those for the central peak in the isotopomer pattern.

Results and Discussion

Initial Considerations. The present work examined fragmentation of a range of polyoxotungstate cluster anions that were transferred to the gas phase by the electrospray process and are closely related to well-defined solution-phase species. For simplicity of notation, hydroxo protons are represented by H in the stoichiometric formulas. For example, the ion cluster $\{Na_2^+[PW_{11}O_{37}(OH)]\}^{2-}$ is represented as $\{Na_2H[PW_{11}O_{38}]\}^{2-}$.

Previous studies[22−27,32−34] reported that numerous species are usually observed from the dissolved salts of a single precursor anion. These were generated as a result of (i) ion pairing leading to ion clusters comprising multiply charged polyoxoanions and different numbers and types of counter cations, (ii) multiple protonation accompanied by a loss of neutral water, and (iii) other chemical transformations induced by changes in pH or concentration as part of the desolvation process during ESI. For example, the spectrum generated from $K_6[P_2W_{18}O_{62}]$ in the present work is shown in Figure 2. The observed ions can be assigned to a range of different species arising from (i) varying numbers of counterions and thus charge (e.g., $\{K[P_2W_{18}O_{62}]\}^{5-}$, $\{K_2[P_2W_{18}O_{62}]\}^{4-}$, and $\{K_3[P_2W_{18}O_{62}]\}^{3-}$ are all observed), (ii) varying contents of K^+ and H^+ (e.g., $\{H_2[P_2W_{18}O_{62}]\}^{4-}$, $\{HK[P_2W_{18}O_{62}]\}^{4-}$, and $\{K_2[P_2W_{18}O_{62}]\}^{4-}$ are all observed), and (iii) ions generated via loss of water from multiply protonated species (e.g., $\{H_2[P_2W_{18}O_{62}]\}^{4-}$ and $[P_2W_{18}O_{61}]^{4-}$ are both observed). Here, we focus essentially on the CID reactions of bare, multiply charged anions that do not contain H^+ or K^+. These bare ions were chosen as ions that contained multiple protons or counterions and were observed to first dissociate via loss of small neutral molecules, for example, H_2O or KOH, to first generate the bare ions, which then undergwent further fragmentation. Fragmentor energy voltages were chosen to maximize gas-phase yields of these bare precursor ions. As a result, fragmentor energy voltages vary

(36) Brevard, C.; Schimpf, R.; Tourné, G.; Tourné, C. M. *J. Am. Chem. Soc.* **1983**, *105*, 7059–7063.
(37) Weakley, T. J. R. *J. Chem. Soc., Dalton Trans.* **1973**, 341–346.
(38) Weakley, T. J. R.; Malik, S. A. *J. Inorg. Nucl. Chem.* **1967**, *29*, 2935–2944.
(39) Tourné, C.; Tourné, G.; Malik, S. A.; Weakley, T. J. R. *J. Inorg. Nucl. Chem* **1970**, *32*, 3875–3890.
(40) Zonnevijlle, F.; Tourné, C. M.; Tourné, G. F. *Inorg. Chem.* **1982**, *21*, 2751–2757.
(41) Finke, R. G.; Droege, M. W.; Domaille, P. J. *Inorg. Chem.* **1987**, *26*, 3886–3896.
(42) Lyon, D. K.; Miller, W. K.; Novet, T.; Domaille, P. J.; Evitt, E.; Johnson, D. C.; Finke, R. G. *J. Am. Chem. Soc.* **1991**, *113*, 7209–7221.

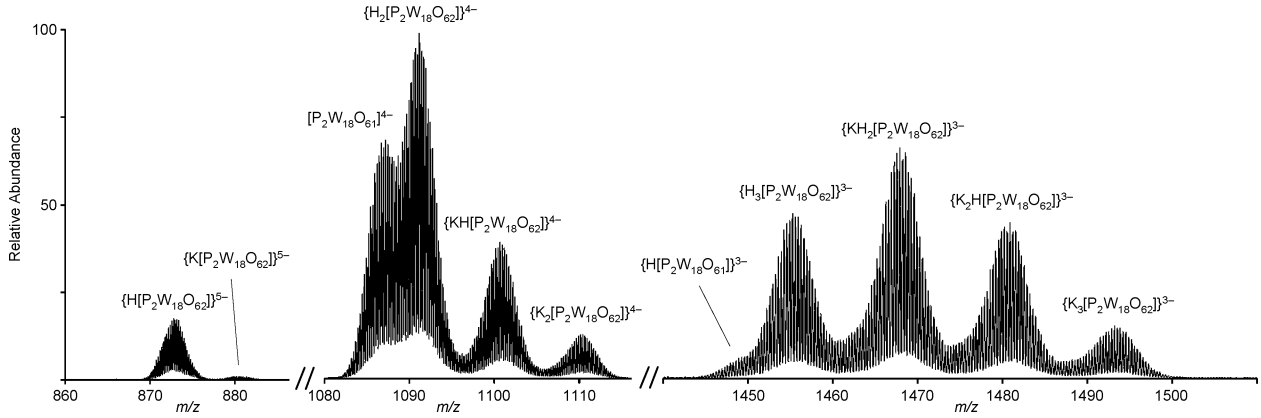

Figure 2. Electrospray mass spectrum of $K_6[P_2W_{18}O_{62}]$ showing a series of ions in the 3^-, 4^-, and 5^- regions arising from the addition of cations H^+ or K^+ to the precursor anion $[P_2W_{18}O_{62}]^{6-}$ as well as the loss of H_2O from multiply protonated species.

from 120 to 170 V. Collision energy voltages used in this study were chosen because they produced CID spectra that satisfied the following requirements: (i) The precursor ion species actually undergoes CID so that the precursor ion's signal is not the most prominent in the CID spectrum. (Low collision voltages produce spectra containing only the precursor ion signals.) (ii) Product ions with low signal intensity can still be easily distinguished from the baseline and confidently assigned. (iii) Product ions produced in the CID process do not undergo further fragmentation before detection. (High collision voltages produce species with low *m*/*z* values. Signals for product ions with higher *m*/*z* values disappear from the spectrum.) Figure S2 illustrates the effect of varying the collision energy voltage (see the Supporting Information). The series of ions studied is summarized in Scheme 1.

The $H_3[PW_{12}O_{40}]$ System. The major ions observed were $[PW_{12}O_{40}]^{3-}$ and $\{H[PW_{12}O_{40}]\}^{2-}$, consistent with previous studies.[35,43] Fragmentation of $[PW_{12}O_{40}]^{3-}$ yielded a series of pairs of complementary ions, each pair comprising a dianionic isopolytungstate $[W_xO_{3x+1}]^{2-}$ and a monoanionic heteropolytungstate $[PW_{12-x}O_{39-3x}]^-$ ($x = 6-9$; Figure 3a; eq 1).

$$[PW_{12}O_{40}]^{3-} \rightarrow [W_6O_{19}]^{2-} + [PW_6O_{21}]^- \quad (1a)$$

$$[PW_{12}O_{40}]^{3-} \rightarrow [W_7O_{22}]^{2-} + [PW_5O_{18}]^- \quad (1b)$$

$$[PW_{12}O_{40}]^{3-} \rightarrow [W_8O_{25}]^{2-} + [PW_4O_{15}]^- \quad (1c)$$

$$[PW_{12}O_{40}]^{3-} \rightarrow [W_9O_{28}]^{2-} + [PW_3O_{12}]^- \quad (1d)$$

The total stoichiometry and charge of each pair of complementary product ions matched those of the precursor anion $[PW_{12}O_{40}]^{3-}$. For example, the most intense product ion $[W_6O_{19}]^{2-}$ (*m*/*z* 704) and its complementary ion $[PW_6O_{21}]^-$ (*m*/*z* 1470) formed one pair, and together they account for the total charge and stoichiometry of $[PW_{12}O_{40}]^{3-}$ (Figure 3a; eq 1a). The pathways producing other pairs of complementary anions are identified in Figure 3a and summarized in eqs 1b−1d. Each of the tungsten and phosphorus atoms in the product species may be assigned as W^{VI} and P^V, respectively, the oxidation states in the precursor ion $[PW_{12}O_{40}]^{3-}$.

The heteropolytungstate products belong to the stoichometric series $[PW_xO_{3x+3}]^-$ ($x = 3-6$; eq 1a). The fragments $[PW_6O_{21}]^-$ and $[PW_3O_{12}]^-$ are the most intense of this series and are also frequently observed as product species of high relative yields from a range of different polyoxotungstate sources (see below). This suggested that they might adopt relatively more stable structures. Their structures are unknown, but cyclic species based on $[(WO_3)_xPO_3]^-$ are appealing possibilities. For example, neutral W_3O_9 is a major component of WO_3 vapors and is known to form a stable ring structure from three corner-sharing WO_4 tetrahedra.[44−46] Insertion of a PO_3^- fragment into the W_3O_9 ring provides a valence-satisfied anion $[(WO_3)_3PO_3]^-$ based upon four corner-sharing tetrahedra. Similarly, the second most intense heteropolytungstate fragment $[PW_6O_{21}]^-$ may be $[(WO_3)_6PO_3]^-$, based upon seven corner-sharing tetrahedra.

The ion produced in highest relative yield is $[W_6O_{19}]^{2-}$, whose stoichiometry matches that of the Lindquist anion, a well-known species that has been characterized in the solid state.[1] The present data cannot distinguish between this structure and the linear alternative $[W_xO_{3x+1}]^{2-}$ ($x = 6$) based upon edge- and corner-shared WO_4 tetrahedra, which have been proposed previously for related species.[14,16] However, the high relative yield of $[W_6O_{19}]^{2-}$ is consistent with it being a relatively stable product under the conditions. The other three isopolytungstate products also belong to the stoichometric series $[W_xO_{3x+1}]^{2-}$ with $x = 7-9$. Again, these might be linear polymers or more complex cluster systems.

Lower mass fragment ions assigned to $[W_xO_{3x+1}]^{2-}$ ($x = 3-5$) as well as $[PW_2O_9]^-$ were also observed. However, the corresponding complementary ions for these species were absent, suggesting that these species were likely formed by additional neutral losses (WO_3, W_2O_6, etc.) from primary fragment ions such as $[W_7O_{22}]^{2-}$ and $[PW_3O_{12}]^-$, respectively. Similar phospho-polytungstate decomposition products have been observed in previous gas-phase studies.[33] Finally,

(43) Tuoi, J. L. Q.; Müller, E. *Rapid Commun. Mass Spectrom.* **1994**, *8*, 692–694.
(44) Ivanov, A. A.; Demidov, A. V.; Popenko, N. I.; Zasorin, E. Z.; Spiridonov, V. P.; Hargittai, I. *J. Mol. Struct.* **1980**, *63*, 121–125.
(45) Huang, X.; Zhai, H.-J.; Kiran, B.; Wang, L.-S. *Angew. Chem., Int. Ed.* **2005**, *44*, 7251–7254.
(46) Li, S.; Dixon David, A. *J. Phys. Chem. A* **2006**, *110*, 6231–6244.

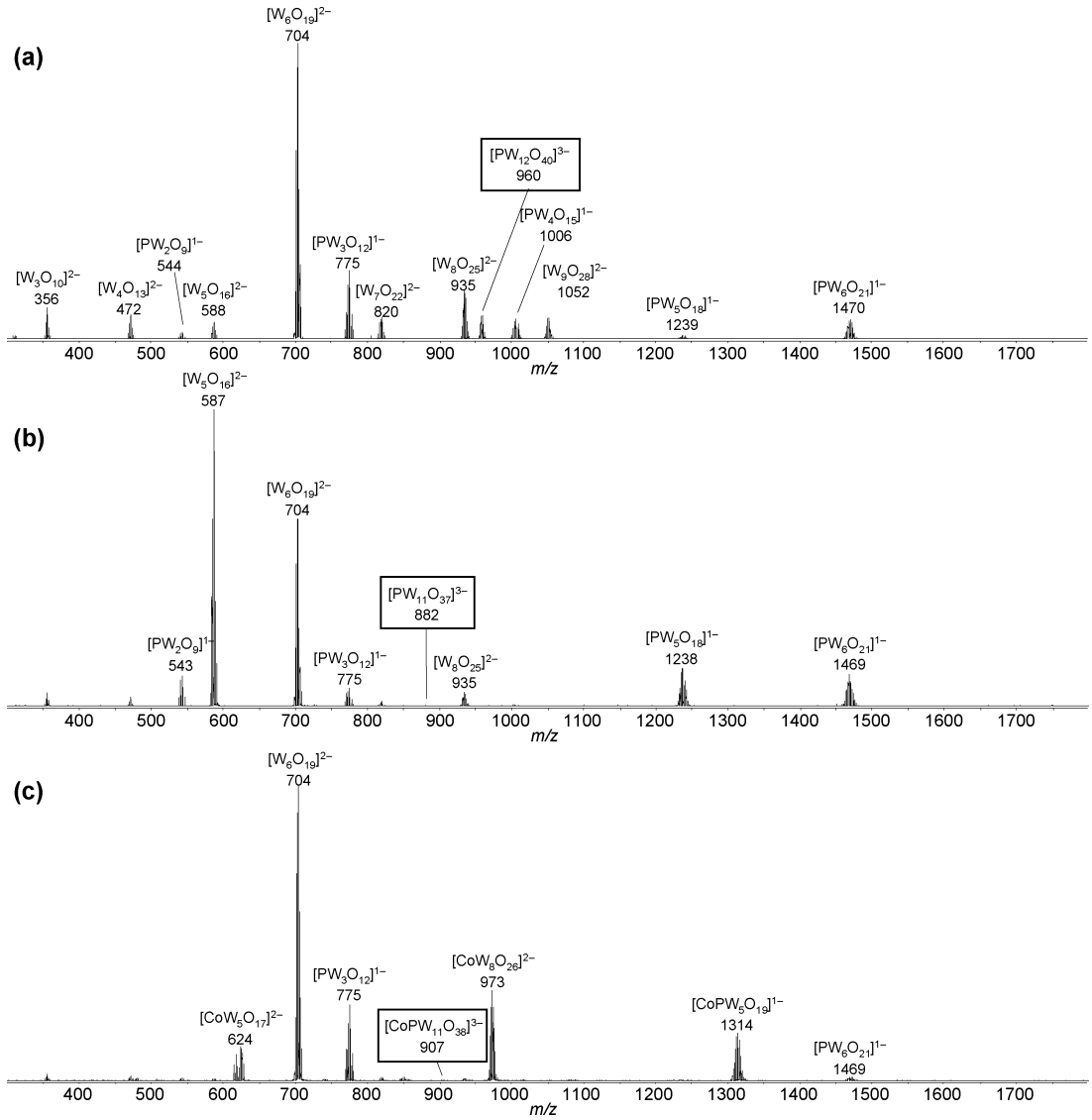

Figure 3. CID mass spectra of (a) the parent Keggin anion $[PW_{12}O_{40}]^{3-}$, (b) the lacunary Keggin anion $[PW_{11}O_{37}]^{3-}$, and (c) the Co^{II}-substituted lacunary Keggin anion $[Co^{II}PW_{11}O_{38}]^{3-}$. The precursor ion in each case is shown in a gray box.

a loss of neutral fragments from $[PW_{12}O_{40}]^{3-}$ was not observed, consistent with fragmentation being driven, at least in part, by the Coulombic repulsion present in the desolvated precursor ion.[31]

The assignment of the product ion at *m*/*z* 704 as $[W_6O_{19}]^{2-}$ differs from that proposed in two previous studies, where the ion was assigned to $[PW_9O_{26}]^{3-}$, which has a similar theoretical *m*/*z* value (*m*/*z* 701) but a different charge.[35,47] The present assignment is supported by the observed isotope peak spacing of 0.5 *m*/*z* units and the close agreement with experimental and theoretical isotope patterns from the high resolving power of the Q-TOF instrument (Figure S1, Supporting Information). On this basis, the assigned stoichiometries of fragmentation products derived from $[PW_{12}O_{40}]^{3-}$ and other Keggion ions studied in the earlier work appear to be incorrect.[35,47]

The $Na_7[PW_{11}O_{39}]$ System. ^{31}P NMR experiments have suggested that the lacunary anion $[PW_{11}O_{39}]^{7-}$ exists as $[PW_{11}O_{36}(OH)_3]^{4-}$ in solution.[48,49] It is formally derived from the precursor Keggin ion $[PW_{12}O_{40}]^{3-}$ by removal of a WO^{4+} fragment and protonation of oxo ligands in the vicinity of the lacunary site. Accordingly, the observation of $[PW_{11}O_{37}]^{3-}$ from the ESI-MS spectra of aqueous solutions of $Na_7[PW_{11}O_{39}]$ is consistent with protonation and a loss of water during ESI (eq 2).

$$[PW_{11}O_{36}(OH)_3]^{4-} + H^+ \rightarrow [PW_{11}O_{35}(OH)_4]^{3-} \rightarrow [PW_{11}O_{37}]^{3-} + 2H_2O \quad (2)$$

The observed anion $[PW_{11}O_{37}]^{3-}$ can be formally derived from the Keggin anion $[PW_{12}O_{40}]^{3-}$ by the removal of a neutral WO_3 unit (Scheme 1), and so its fragmentation pathways were examined for comparison with $[PW_{12}O_{40}]^{3-}$ (eq 1a). Fragmentation occurred by two major pathways to produce the two complementary pairs of ions $\{[W_5O_{16}]^{2-}, [PW_6O_{21}]^-\}$ and $\{[W_6O_{19}]^{2-}, [PW_5O_{18}]^-\}$ (Figure 3b; eqs

(47) Bonchio, M.; Bortolini, O.; Conte, V.; Sartorel, A. *Eur. J. Inorg. Chem.* **2003**, 699–704.

(48) Combs-Walker, L. A.; Hill, C. L. *Inorg. Chem.* **1991**, *30*, 4016–4026.

(49) Dablemont, C.; Proust, A.; Thouvenot, R.; Afonso, C.; Fournier, F.; Tabet, J.-C. *Inorg. Chem.* **2004**, *43*, 3514–3520.

3a and 3b). A much weaker signal was also observed for the complementary pair $\{[W_8O_{25}]^{2-}, [PW_3O_{12}]^-\}$ (eq 3c). Each of the complementary pairs again add to give the total stoichiometry and charge of the precursor ion $[PW_{11}O_{37}]^{3-}$.

$$[PW_{11}O_{37}]^{3-} \rightarrow [W_5O_{16}]^{2-} + [PW_6O_{21}]^- \quad (3a)$$

$$[PW_{11}O_{37}]^{3-} \rightarrow [W_6O_{19}]^{2-} + [PW_5O_{18}]^- \quad (3b)$$

$$[PW_{11}O_{37}]^{3-} \rightarrow [W_8O_{25}]^{2-} + [PW_3O_{12}]^- \quad (3c)$$

The natures of the fragment ions observed are similar to those observed for $[PW_{12}O_{40}]^{3-}$ (eq 1a), that is, a dianionic isopolytungstate and a monoanionic heteropolytungstate. Formation of the pair $\{[W_6O_{19}]^{2-}, [PW_5O_{18}]^-\}$ is presumably driven by the known stability of $[W_6O_{19}]^{2-}$ (eq 3b). In contrast, neither of the products $\{[W_5O_{16}]^{2-}, [PW_6O_{21}]^-\}$ in the other intense channel are known condensed-phase species (eq 3a). However, $[PW_6O_{21}]^-$ is observed in CID experiments on a range of polyoxotungstate species, suggesting that it might be a relatively stable fragment ion (see, e.g., eq 1a and discussion below).

The $K_5[(H_2O)MPW_{11}O_{39}]$ ($M = Co^{II}$, Ni^{II}, Cu^{II}) Systems. The anion $[CoPW_{11}O_{38}]^{3-}$ was observed from the ESI of an aqueous solution of $K_5[(H_2O)CoPW_{11}O_{39}]$ and presumably formed by protonation and a loss of water from the precursor ion $[CoPW_{11}O_{39}]^{5-}$. It is related to the lacunary anion $[PW_{11}O_{37}]^{3-}$ discussed above by the formal addition of neutral CoO, and to the Keggin anion $[PW_{12}O_{40}]^{3-}$ by the removal of WO_3 and the addition of CoO (Scheme 1). $[CoPW_{11}O_{38}]^{3-}$ fragmented via two pathways, both of which again gave pairs of complementary anions (Figure 3c; eq 4a). The pathways differ in the final location of the Co and P atoms across the two species within each pair. In the first one, Co and P are retained on the same product ion, $[CoPW_5O_{19}]^-$, and the complementary ion is $[W_6O_{19}]^{2-}$ (eq 4a). In the second pathway, Co and P are retained on different product ions, and two complementary pairs of ions are produced, $\{[CoW_5O_{17}]^{2-}, [PW_6O_{21}]^-\}$ and $\{[CoW_8O_{26}]^{2-}, [PW_3O_{12}]^-\}$ (eqs 4b and 4c). The fragments generated in the second pathway differ by a neutral W_3O_9 unit, that is, $[Co^{II}W_5O_{17}]^{2-}$, $[Co^{II}W_8O_{26}]^{2-}$ and $[PW_6O_{21}]^-$, $[PW_3O_{12}]^-$ (eqs 4b and 4c). This is again consistent with the known stability of neutral W_3O_9.[44−46]

$$[Co^{II}PW_{11}O_{38}]^{3-} \rightarrow [Co^{II}PW_5O_{19}]^- + [W_6O_{19}]^{2-} \quad (4a)$$

$$[Co^{II}PW_{11}O_{38}]^{3-} \rightarrow [Co^{II}W_5O_{17}]^{2-} + [PW_6O_{21}]^- \quad (4b)$$

$$[Co^{II}PW_{11}O_{38}]^{3-} \rightarrow [Co^{II}W_8O_{26}]^{2-} + [PW_3O_{12}]^- \quad (4c)$$

The distribution of phosphorus and tungsten in fragmentation products from $[Co^{II}PW_{11}O_{38}]^{3-}$ is equivalent to that from related species $[PW_{11}O_{37}]^{3-}$, with products differing only due to the presence of the additional CoO in the former (compare eqs 3a and 4a). For example, in the first pathway, the additional CoO is retained on the $[PW_5O_{18}]^-$ fragment to give the complementary pair $\{[Co^{II}PW_5O_{19}]^-, [W_6O_{19}]^{2-}\}$, presumably due to the stability of $[W_6O_{19}]^{2-}$ (compare eqs 4a and 3b). In contrast, the additional CoO is retained on the other fragment in the other pathways, giving rise to the complementary pairs $\{[Co^{II}W_5O_{17}]^{2-}, [PW_6O_{21}]^-\}$ and $\{[Co^{II}W_8O_{26}]^{2-}, [PW_3O_{12}]^-\}$ (compare eqs 4b and 4c with 3a and 3c, respectively). These second pathways are presumably driven by the formation of the relatively stable anions $[PW_6O_{21}]^-$ and $[PW_3O_{12}]^-$, which are observed in the present work as fragmentation products from a wide range of clusters.

Analogous CID pathways were observed for $[Ni^{II}PW_{11}O_{38}]^{3-}$ and $[Cu^{II}PW_{11}O_{38}]^{3-}$ (Figure S3, Supporting Information). The observed *m*/*z* shifts with variation of M = Co, Ni, and Cu can be attributed to the different molecular masses of the third row transition metal atoms. This aspect supports the fragment assignments given above.

$K_4[(H_2O)FePW_{11}O_{39}]$ and Derivatives. The dianion $[FePW_{11}O_{38}]^{2-}$ was observed from ESI-MS of solutions of $K_4[(H_2O)FePW_{11}O_{39}]$ and is presumably formed by protonation and a loss of water from the precursor ion $[FePW_{11}O_{39}]^{4-}$ during the electrospray process (eq 5). It is related to the lacunary anion $[PW_{11}O_{37}]^{3-}$ described above by the formal addition of FeO^+ to $[PW_{11}O_{37}]^{3-}$, and to $[CoPW_{11}O_{38}]^{3-}$ by the substitution of Fe^{III} for Co^{II} (giving rise to a dianion rather than a trianion).

$$[FePW_{11}O_{39}]^{4-} + 2H^+ \rightarrow [FePW_{11}O_{38}]^{2-} + H_2O \quad (5)$$

The fragmentation pathways of $[FePW_{11}O_{38}]^{2-}$ are summarized in eq 6 (Figure S4, Supporting Information). The observed fragments are similar to those seen for $[Co^{II}PW_{11}O_{38}]^{3-}$ (eq 4a), except that the presence of Fe^{III} means that the $[MW_xO_{3x+2}]^{n-}$ fragments are monoanionic rather than dianionic.

$$[Fe^{III}PW_{11}O_{38}]^{2-} \rightarrow [FeW_xO_{3x+2}]^- + [PW_{11-x}O_{36-3x}]^- \quad (x = 3-8) \quad (6)$$

A pathway analogous to eq 4a for $[Co^{II}PW_{11}O_{38}]^{3-}$ giving rise to $\{[Co^{II}PW_5O_{19}]^-, [W_6O_{19}]^{2-}\}$is not observed for $[Fe^{III}PW_{11}O_{38}]^{2-}$. The analogous product $[Fe^{III}PW_5O_{19}]$ would be neutral and thus would not be observed. However, the absence of the complementary product $[W_6O_{19}]^{2-}$suggests that this pathway does not occur. The two most dominant fragmentation pathways are again for $x = 5$ and $x = 8$, as observed for $[Co^{II}PW_{11}O_{38}]^{3-}$ (eqs 4b and 4c). These again give rise to pairs of fragments featuring $[PW_6O_{21}]^-$ ($x = 5$) or $[PW_3O_{12}]^-$ ($x = 8$), identified earlier.

The $K_6[P_2W_{18}O_{62}]$ System. The anion $[P_2W_{18}O_{61}]^{4-}$ was observed (Figure 2) and is again presumably formed as a result of protonation and a loss of water from the precursor ion $[P_2W_{18}O_{61}]^{6-}$ (eq 7).

$$[P_2W_{18}O_{62}]^{6-} + 2H^+ \rightarrow [P_2W_{18}O_{60}(OH)_2]^{4-} \rightarrow [P_2W_{18}O_{61}]^{4-} + H_2O \quad (7)$$

Fragmentation of $[P_2W_{18}O_{61}]^{4-}$ occurred along two pathways, which differed in the location of the two phosphorus heteroatoms (Figure 4a, eq 8a). The first involved the formation of complementary pairs of isopolyanions $[W_xO_{3x+1}]^{2-}$ and heteropolyanions $[P_2W_{18-x}O_{60-3x}]^{2-}$ (eq 8a, $x = 4-6$). Both phosphorus atoms are localized in the second fragment ion, and this pathway was observed for $x = 4-6$.

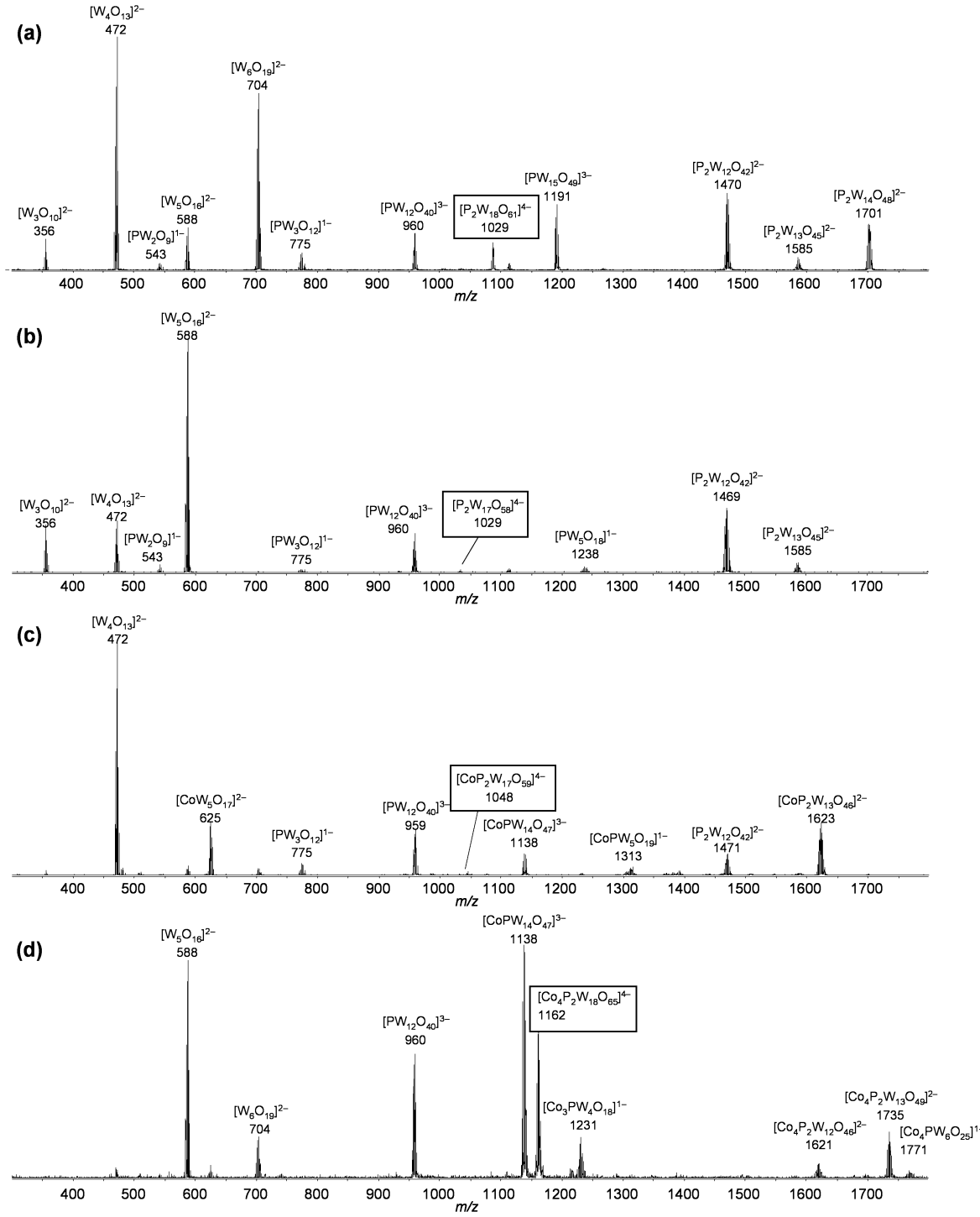

Figure 4. CID mass spectra of (a) the parent Dawson anion $[P_2W_{18}O_{61}]^{4-}$, (b) the lacunary Dawson anion $[P_2W_{17}O_{58}]^{4-}$, (c) the Co^{II}-substituted Dawson anion $[Co^{II}P_2W_{17}O_{59}]^{4-}$, and (d) the Co^{II}-containing sandwich anion $[Co_4P_2W_{18}O_{65}]^{4-}$. The precursor ion in each case is shown in a gray box.

The second pathway generated the pair of heteropolyanions $\{[PW_{15}O_{49}]^{3-}, [PW_3O_{12}]^{-}\}$ with one phosphorus atom in each fragment (eq 8b). Again, the relatively stable anion $[PW_3O_{12}]^{-}$ appeared.

$$[P_2W_{18}O_{61}]^{4-} \rightarrow [W_xO_{3x+1}]^{2-} + [P_2W_{18-x}O_{60-3x}]^{2-} \quad (x = 4-6) \quad (8a)$$

$$[P_2W_{18}O_{61}]^{4-} \rightarrow [PW_{15}O_{49}]^{3-} + [PW_3O_{12}]^{-} \quad (8b)$$

A fragment ion of stoichiometry $[PW_{12}O_{40}]^{3-}$ was also observed (Figure 4a), whose molecular formula matches that of the well-known Keggin anion. The expected complementary product anion is $[PW_6O_{21}]^{-}$, which has an identical *m*/*z* value to that of the experimentally observed anion $[P_2W_{12}O_{42}]^{2-}$. However, the experimentally observed isotope pattern for $[P_2W_{12}O_{42}]^{2-}$ does not indicate the presence of singly charged $[PW_6O_{21}]^{-}$ at identical *m*/*z* values, suggesting that $[PW_6O_{21}]^{-}$ is not formed experimentally (Figure S5, Supporting Information). This indicated that product $[PW_{12}O_{40}]^{3-}$ is generated in a different pathway, perhaps via loss of the stable neutral unit W_3O_9 from $[PW_{15}O_{49}]^{3-}$.

The $K_{10}[P_2W_{17}O_{61}]$ System. This lacunary system also displayed anions based on $[P_2W_{17}O_{59}]^{6-}$ and $[P_2W_{17}O_{58}]^{4-}$, both presumably formed via loss of two or three water molecules, respectively, from protonated forms of the precursor ion $[P_2W_{17}O_{61}]^{10-}$. $[P_2W_{17}O_{58}]^{4-}$ was examined by CID, and two major fragmentation pathways were present (Figure 5b, eq 9a). The first pathway was equivalent to that described above for the intact Dawson anion $[P_2W_{18}O_{61}]^{4-}$ and involved the formation of complementary pairs of isopolyanions $[W_xO_{3x+1}]^{2-}$ and heteropolyanions $[P_2W_{17-x}O_{57-3x}]^{2-}$ (eqs 9a and 9b; $x = 4, 5$). Both phosphorus heteroatoms were retained on the larger fragments $[P_2W_{13}O_{45}]^{2-}$ and $[P_2W_{12}O_{42}]^{2-}$, formed with complementary isopolyanions $[W_4O_{13}]^{2-}$ and $[W_5O_{16}]^{2-}$, respectively (eqs 9a and 9b). The second fragmentation pathway involved the formation of $[PW_{12}O_{40}]^{3-}$ and the complementary ion $[PW_5O_{18}]^{-}$ (eq 9c). The observation of a gas-phase species with the same stoichiometry as the Keggin anion is interesting given the known condensed-phase stability of $[PW_{12}O_{40}]^{3-}$.

$$[P_2W_{17}O_{58}]^{4-} \rightarrow [W_4O_{13}]^{2-} + [P_2W_{13}O_{45}]^{2-} \quad (9a)$$

$$[P_2W_{17}O_{58}]^{4-} \rightarrow [W_5O_{16}]^{2-} + [P_2W_{12}O_{42}]^{2-} \quad (9b)$$

$$[P_2W_{17}O_{58}]^{4-} \rightarrow [PW_{12}O_{40}]^{3-} + [PW_5O_{18}]^{-} \quad (9c)$$

The $K_8[(H_2O)MP_2W_{17}O_{61}]$ Systems ($M = Co^{2+}$, Ni^{2+}, Cu^{2+}). $[CoP_2W_{17}O_{59}]^{4-}$ was observed in the mass spectrum of $K_8[(H_2O)CoP_2W_{17}O_{61}]$ and is presumably formed via protonation and a loss of water from the precursor ion $[CoP_2W_{17}O_{61}]^{8-}$. Fragmentation of $[CoP_2W_{17}O_{59}]^{4-}$ is more complex, as the presence of a cobalt and two phosphorus atoms allows a more complex distribution of these atoms across the complementary fragment ions (Figure 4c; eq 10a). Both of the phosphorus atoms were retained on the same fragment ion in channels 10a and 10b, but on different fragments in channels 10c and 10d.

$$[CoP_2W_{17}O_{59}]^{4-} \rightarrow [W_4O_{13}]^{2-} + [CoP_2W_{13}O_{46}]^{2-} \quad (10a)$$

$$[CoP_2W_{17}O_{59}]^{4-} \rightarrow [CoW_5O_{17}]^{2-} + [P_2W_{12}O_{42}]^{2-} \quad (10b)$$

$$[CoP_2W_{17}O_{59}]^{4-} \rightarrow [CoPW_5O_{19}]^{-} + [PW_{12}O_{40}]^{3-} \quad (10c)$$

$$[CoP_2W_{17}O_{59}]^{4-} \rightarrow [PW_3O_{12}]^{-} + [CoPW_{14}O_{47}]^{3-} \quad (10d)$$

Fragmentation to produce $[W_4O_{13}]^{2-}$ and $[CoP_2W_{13}O_{46}]^{2-}$ (eq 10a) is related to that observed for the lacunary Dawson anion $[P_2W_{17}O_{58}]^{4-}$ to produce $[W_4O_{13}]^{2-}$ and $[P_2W_{13}O_{45}]^{2-}$ (eq 9a). $[W_4O_{13}]^{2-}$ is formed in each case with the additional CoO in $[CoP_2W_{17}O_{59}]^{4-}$ retained on the second fragment to give $[CoP_2W_{13}O_{46}]^{2-}$ rather than $[P_2W_{13}O_{45}]^{2-}$. Similarly, the fragmentation pathway observed for $[CoP_2W_{17}O_{59}]^{4-}$ in eq 10b to yield $[CoW_5O_{17}]^{2-}$ and $[P_2W_{12}O_{42}]^{2-}$ is related to that observed for $[P_2W_{17}O_{58}]^{4-}$ to give $[W_5O_{16}]^{2-}$ and $[P_2W_{12}O_{42}]^{2-}$ (eq 9b). Both pathways produce $[P_2W_{12}O_{42}]^{2-}$, and the additional CoO in $[CoP_2W_{17}O_{59}]^{4-}$ is retained on the complementary product ion to give $[CoW_5O_{17}]^{2-}$ rather than $[W_5O_{16}]^{2-}$. Finally, the fragmentation pathways observed in eqs 9c and 10c both produced $[PW_{12}O_{40}]^{3-}$. The complementary ion for $[P_2W_{17}O_{58}]^{4-}$ was $[PW_5O_{18}]^{-}$ (eq 9c), while that for $[CoP_2W_{17}O_{59}]^{4-}$ was $[CoPW_5O_{19}]^{-}$ (eq 10c) due to the additional CoO in the latter.

Analogous fragmentation pathways were observed for $[NiP_2W_{17}O_{59}]^{4-}$ and $[CuP_2W_{17}O_{59}]^{4-}$, with the observed m/z shifts with variation of M = Co, Ni, and Cu again supporting the fragment assignments given above (Figure S6, Supporting Information).

The $K_{10}[(H_2O)_2Co_4(PW_9O_{34})_2]$ System. An anion of stoichiometry $[Co_4P_2W_{18}O_{65}]^{4-}$ was observed, again presumably formed via protonation and a loss of water from the precursor ion $[Co_4(PW_9O_{34})_2]^{10-}$. $[Co_4P_2W_{18}O_{65}]^{4-}$ again fragmented to produce complementary pairs of product anions (Figure 4d; eq 11a).

$$[Co_4P_2W_{18}O_{65}]^{4-} \rightarrow [W_5O_{16}]^{2-} + [Co_4P_2W_{13}O_{49}]^{2-} \quad (11a)$$

$$[Co_4P_2W_{18}O_{65}]^{4-} \rightarrow [W_6O_{19}]^{2-} + [Co_4P_2W_{12}O_{46}]^{2-} \quad (11b)$$

$$[Co_4P_2W_{18}O_{65}]^{4-} \rightarrow [PW_{12}O_{40}]^{3-} + [Co_4PW_6O_{25}]^{-} \quad (11c)$$

$$[Co_4P_2W_{18}O_{65}]^{4-} \rightarrow [CoPW_{14}O_{47}]^{3-} + [Co_3PW_4O_{18}]^{-} \quad (11d)$$

Pathways 11a and 11b can be compared to those of the intact Dawson species (eq 8a) where $[W_5O_{16}]^{2-}$ and $[W_6O_{19}]^{2-}$ were formed. Here, the complementary fragment ions, $[Co_4P_2W_{13}O_{49}]^{2-}$ and $[Co_4P_2W_{12}O_{46}]^{2-}$, differ from those in the intact Dawson series by formal addition of the four CoO units. All four Co^{2+} ions and the two phosphorus heteroatoms are retained on the same fragment (eqs 11a and 11b). $[PW_{12}O_{40}]^{3-}$ was observed in a fragmentation pathway of $[Co_4P_2W_{18}O_{65}]^{4-}$ (eq 11c). The precursor sandwich compound consists of two PW_9 units separated by a "raft" of four cobalt ions (Figure 1d). Therefore, it is expected that the formation of a fragment ion containing more than nine tungsten atoms and no cobalt ions would require considerable rearrangement, and so it is of interest that $[PW_{12}O_{40}]^{3-}$ is present as a fragment ion here. This is further evidence that a species with the same stoichiometry as a Keggin ion acts as a thermodynamic sink in the gas phase. The complementary fragment ion $[Co_4PW_6O_{25}]^{-}$ retains all four Co^{2+} ions and differs from the commonly observed ion $[PW_6O_{21}]^{-}$ discussed above (e.g., eqs 1a and 3a) by the formal addition of four CoO units.

The signal corresponding to $[CoPW_{14}O_{47}]^{3-}$ is one of the most intense peaks in the CID spectrum of $[Co_4P_2W_{18}O_{65}]^{4-}$ (Figure 4d, eq 11d), and the complementary ion $[Co_3PW_4O_{18}]^{-}$ is also observed, albeit at lower intensity. $[CoPW_{14}O_{47}]^{3-}$ is also observed in the CID spectrum of the

metal-substituted Dawson anion $[CoP_2W_{17}O_{59}]^{4-}$, where its complementary fragment is $[PW_3O_{12}]^-$ (eq 10d).

Analogous CID pathways were observed for $[Zn_4P_2W_{18}O_{65}]^{4-}$ (Figure S6, Supporting Information). The observed m/z shifts with variation of M = Co or Zn can be attributed to the different molecular masses of the first row transition metal atoms and were used to support the assignment of observed fragments.

Conclusions

A range of classic phospho-polyoxotungstate anions based upon Keggin $[PW_{12}O_{40}]^{3-}$, Dawson $[P_2W_{18}O_{62}]^{6-}$, and Tourné $[Co_4P_2W_{18}O_{68}]^{10-}$ clusters, as well as their lacunary and metal-substituted derivatives, were transferred to the gas phase by electrospray ionization. In each case, species closely related to the condensed-phase precursor ion were mass-selected and their fragmentation examined by collision-induced dissociation (Scheme 1).

A common feature of the fragmentation of different clusters was the observation of multiple reaction channels leading to pairs of complementary product anions whose total stoichiometry and charge matched those of the precursor anion. For example, $[PW_{12}O_{40}]^{3-}$ fragmented to give pairs of product ions comprised of a dianionic isopolytungstate $[W_xO_{3x+1}]^{2-}$ and a monoanionic heteropolytugstate $[PW_{12-x}O_{39-3x}]^-$ ($x = 6-9$), with the most intense pair being $[W_6O_{19}]^{2-}$ and $[PW_6O_{21}]^-$. The total stoichiometry and charge of each pair matched that of the precursor anion $[PW_{12}O_{40}]^{3-}$.

Clusters of stoichiometries matching those of well-known condensed-phase species were commonly observed as fragment ions; for example, $[W_6O_{19}]^{2-}$ and $[PW_{12}O_{40}]^{3-}$ were observed as fragments from larger clusters such as $[P_2W_{18}O_{61}]^{3-}$ and $[Co_4P_2W_{18}O_{65}]^{4-}$. However, it is unknown whether these fragment ions adopt equivalent structures to their condensed-phase counterparts. Nevertheless, the observation of these fragment ions is striking and is consistent with these stable condensed-phase species also representing stable thermodynamic sinks in gas-phase fragmentation processes.

Heteropolytungstate ions such as $[PW_3O_{11}]^-$ and $[PW_6O_{21}]^-$ were observed as common intense fragment ions from a range of different sources. These ions do not appear to have known condensed-phase analogues, but their gas-phase stability suggests they might also adopt stable structures. Valence-satisfied rings based upon corner-sharing tetrahedra (analogous to W_3O_9) are intuitively appealing structures.

The present work is useful in further defining the scope of electrospray ionization and collision-induced dissociation in the characterization of polyoxotungstate clusters. In particular, the proper documentation of the fragmentation of clusters of known stoichiometry presented here will help with future characterization of clusters whose stoichiometry and structure is unknown.

Acknowledgment. We thank the Australian Research Council for financial support via grants DP0772053 (T.W.), DP0450134 (M.T.M. and A.G.W.) and DP0558430 (R.A.J.O.). We thank the Research Transfer Facility of Bio21 for access to the Agilent 6510 Q-TOF and Paul O'Donnell for helping train two of us (M.T.M. and T.W.) in the use of the instrument.

Supporting Information Available: Additional figures. This material is available free of charge via the Internet at http://pubs.acs.org.

IC8016326